Viral ADP-ribosyltransferases attach RNA chains to host proteins

Katharina Höfer (Katharina.Hoefer@synmikro.mpi-marburg.mpg.de)
Max Planck Institute for terrestrial Microbiology https://orcid.org/0000-0002-7472-9887
Maik Schauerte
Max Planck Institute for terrestrial Microbiology https://orcid.org/0000-0001-6988-2775
Julia Grawenhoff
Institute of Pharmacy and Molecular Biotechnology (IPMB), Heidelberg University
Alexander Wulf
Max Planck Institute for Biophysical Chemistry
Luisa Welp
Max Planck Institute for Biophysical Chemistry
Franziska Billau
Institute of Pharmacy and Molecular Biotechnology (IPMB), Heidelberg University
Henning Urlaub
Max-Planck-Institute https://orcid.org/0000-0003-1837-5233
Andres Jäschke
Heidelberg University https://orcid.org/0000-0002-4625-2655

Biological Sciences - Article

Keywords: Bacteriophage T4, Transcriptional and Translational Apparatus, Covalent RNA Chain Link, Decelerated Lysis, Phage Replication Cycle, Enzymatic Transfer, Post-translational Protein Modification

Posted Date: June 16th, 2021

DOI: https://doi.org/10.21203/rs.3.rs-590309/v1

Version of Record: A version of this preprint was published at Nature on August 16th, 2023. See the published version at https://doi.org/10.1038/s41586-023-06429-2.

Abstract

The mechanisms by which viruses hijack their host's genetic machinery are of enormous current interest. One mechanism is adenosine diphosphate (ADP) ribosylation, where ADP-ribosyltransferases (ARTs) transfer an ADP-ribose fragment from the ubiquitous coenzyme nicotinamide adenine dinucleotide (NAD) to acceptor proteins. When bacteriophage T4 infects Escherichia coli, three different ARTs reprogram the host's transcriptional and translational apparatus. Recently, NAD was identified as a 5'-modification of cellular RNA molecules in bacteria and higher organisms. Here, we report that bacteriophage T4 ARTs accept not only NAD, but also NAD-RNA as substrate, thereby covalently linking entire RNA chains to acceptor proteins in an "RNAylation" reaction. One of these ARTs, ModB, efficiently RNAylates its host protein target, ribosomal protein S1, at arginine residues and strongly prefers NAD-RNA over NAD. Mutation of a single arginine at position 139 abolishes ADP-ribosylation and RNAylation. Overexpression of mammalian ADP-ribosylarginine hydrolase 1 (ARH1), which cleaves arginine-phosphoribose bonds, shows a decelerated lysis of E. coli when infected with T4. Our findings not only challenge the established views of the phage replication cycle, but also reveal a distinct biological role of NAD-RNA, namely activation of the RNA for enzymatic transfer. Our work exemplifies the first direct connection between RNA modification and post-translational protein modification. As ARTs play important roles in different viral infections, as well as in antiviral defence by the host, RNAylation may have far-reaching implications.

Introduction

ARTs catalyse the transfer of one or multiple ADP-ribose (ADPr) units from NAD to target proteins [1]. In bacteria and archaea, they act as toxins, are involved in host defence or drug resistance mechanisms [8], while in eukaryotes, they play roles in distinct processes ranging from DNA damage repair to macrophage activation and stress response [9]. Viruses use ARTs as weapons to reprogram the host's gene expression system [7]. Mechanistically, a nucleophilic group of the target protein (mostly Arg, Glu, Asp, Ser, Cys) attacks the glycosidic carbon atom in the nicotinamide riboside moiety of NAD, forming a covalent bond as N-, O-, or S-glycoside (Fig. 1a) [1]. As the adenosine moiety of NAD is not involved in this reaction, we speculated that elongation of the adenosine to long RNA chains (via regular 5'-3'-phosphodiester bonds) might be tolerated by ARTs, potentially leading to the formation of covalent RNA-protein conjugates (Fig. 1b). RNAs harbouring a 5'-NAD-cap were recently found in bacteria, including *E. coli* [4,10,11], and higher organisms [5,12–14], but very little is known about the biological functions of this RNA cap [15].

The infection cycle of bacteriophage T4 relies on the sequential expression of early, middle and late phage genes that are transcribed by *E. coli* RNA polymerase (RNAP) [16]. For the specific temporal reprogramming of the *E. coli* transcriptional and translational apparatus, the T4 phage uses three ARTs that modify over 30 host proteins: Alt is injected into the bacterium together with the phage DNA and immediately ADP-ribosylates *E. coli* RNAP at different positions, thought to result in the preferential transcription of phage genes from "early" promoters [17,18]. Two early phage genes code for the ARTs

ModA [19] and ModB [2,20]. The former completes ADP-ribosylation of RNAP, while the latter modifies a set of host proteins mostly involved in translation [18]. However, it is still unknown how ADP-ribosylation changes the proteins' properties.

Results

T4 ARTs catalyse RNAylations in vitro

To test our hypothesis that ARTs may accept NAD-RNAs as substrates, we purified the three T4 ARTs and incubated them with a synthetic, site-specifically ^{32}P-labelled 5'-NAD-RNA 8mer to test for either self-modification or modification of target proteins. Modification is indicated by the acquisition of the ^{32}P-label by the ART or the target protein, respectively. While both Alt and ModA showed only a low extent of self- and target RNAylation (Extended Data Fig. 1a), ModB rapidly RNAylated its known target, ribosomal protein S1 (rS1) without detectable self-RNAylation, as indicated by radioactive bands with the expected mobility in SDS-PAGE gels. In contrast, ADP-ribosylation in the presence of ^{32}P-NAD resulted in the modification of both proteins (ModB and rS1) with similar radioactive band intensities (Fig. 2a,b and Extended Data Fig. 1b,c). The radioactive band did not appear when either ModB or rS1 were missing or when a 5'-^{32}P-monophosphate-RNA (5'-^{32}P-RNA) of the same sequence was used as a substrate for ModB (Extended Data Fig. 1d).

ModB prefers NAD-RNA over NAD

ModB-catalysed RNAylation of rS1 was strongly inhibited by the ART inhibitor 3-methoxybenzamide (3-MB) (Extended Data Fig. 2a). The radioactive rS1 band did not disappear when the reaction product was treated with RNase T1. This treatment would remove the ^{32}P-label if the RNA was non-covalently bound to rS1 or was covalently linked via other than 5'-terminal positions (Extended Data Fig. 2b). The bacterial enzyme NudC [21], which hydrolyses pyrophosphate bonds in various non-canonical cap structures, caused a decrease of the radioactive signal by 53 % (Extended Data Fig. 2c), indicating the generation of ribose 5'-phosphate modified rS1. The radioactive band, however, disappeared entirely upon treatment with trypsin (which digests rS1) (Extended Data Fig. 2c). Collectively, these data strongly support the covalent linkage of a RNA to rS1 via a diphosphoriboside linkage as shown in Fig. 1b.

Competition experiments using ^{32}P-NAD-RNA and an excess of unlabeled NAD revealed a preference of ModB for the former, which is important for modification reactions *in vivo*, where NAD is much more abundant than NAD-RNA (Fig. 2c and Extended Data Fig. 3a). ModB also accepted longer, biologically relevant RNAs with comparable activity (e.g., a Qβ-RNA fragment of ~ 100 nt [22], Fig. 2d and Extended Data Fig. 3b). RNAylation with this NAD-capped-Qβ-RNA caused protein rS1 (~ 70 kDa) to move like a 100 kDa protein on an SDS-PAGE gel (Fig. 2e). Treatment of the RNAylated protein with nuclease P1, which hydrolyses 3'-5' phosphodiester bonds but does not attack the pyrophosphate bond of the 5'-ADP-ribose, reverted this shift, and the radioactive product migrated like non-modified rS1 or ADPr-rS1 (Fig. 2e), again confirming the proposed nature of the covalent linkage.

To exclude the possibility that ModB might just remove the nicotinamide moiety from the NAD-RNA by hydrolysis, generating a highly reactive ribosyl moiety that could (via its masked aldehyde group) spontaneously react with nucleophiles in its vicinity [23], we prepared authentic ADP-ribose-modified RNA (site-specifically ^{32}P-labelled) and tested it as substrate. No radioactive band appeared (Extended Data Fig. 3c), providing no support for spontaneous ADP-ribosylation.

ModB modifies specific arginines in rS1

To identify the amino acid residues in protein rS1 to which RNA chains are covalently linked during RNAylation, we took advantage of tools developed to analyse protein ADP-ribosylation. The radioactive signal of RNAylated protein rS1 (as prepared in Fig. 2b) did not change upon treatment with $HgCl_2$ (which cleaves S-glycosides resulting from Cys), NH_2OH (which hydrolyses O-glycosides) (Extended Data Fig. 4a) and recombinant enzyme ARH3 (which hydrolyses O-ADPr glycosides specifically at serine residues) (Extended Data Fig. 4b), while it was efficiently removed by treatment with human ARH1 [24] (Fig. 3a-d). These findings indicate that the major product(s) of the ModB-catalysed RNAylation reaction are linked as N-glycosides via arginine residues (as shown in Fig. 3a,b).

To identify the amino acid residues which are targeted by ModB, *in vitro* modified rS1 was subjected to tryptic digest, chromatographic purification, and mass-spectrometric analysis. This LC/MS/MS analysis revealed three specific modification sites in rS1, namely R19, R139, and R426 (Extended Data Fig. 5).

To establish the biological significance of RNAylation by T4 ARTs *in vivo*, we isolated endogenous (untagged) protein rS1 from non-infected and T4-infected *E. coli*, respectively. *E. coli* contains significant amounts of endogenous NAD-RNAs [4,6]. Ribosomes were isolated, and rS1 was pulled down by poly-U-sepharose and subjected to LC/MS/MS analysis (Fig. 3e). This experiment confirmed the *in vitro* data and revealed the same three sites, namely R19, R139 and R426, at which phosphoribose modifications were abundant only in the T4-infected sample. (Fig. 3f). Site-directed mutagenesis further confirmed the modified residues: R139K and R139A mutants of protein rS1 were expressed in T4-infected *E. coli*, purified and analysed, revealing that these mutations abolish the modification (Extended Data Fig. 6).

Detection of RNAylation in vivo

The mass spectrometric pipeline detected ADP-ribosylation and RNAylation in the same way, namely as ribose-5'-phosphate or ADPr fragment. To distinguish between the two modifications, we considered an immunoblotting assay with an antibody-like ADP-ribose binding reagent ("pan-ADPr"). The specificity of pan-ADPr was investigated by Western blotting with *in vitro*-prepared ADP-ribosylated or RNAylated proteins, respectively (Extended Data Fig. 7a). As expected, rS1-ADPr and ModB-ADPr were both recognised by pan-ADPr and produced bands with high intensities, while no signal was observed for rS1-RNA, suggesting that pan-ADPr does not tolerate 3'-extensions of the ribose moiety. However, when rS1-RNA was digested with nuclease P1 prior to pan-ADPr treatment, thereby degrading the RNA and likely leaving rS1-ADPr, a strong signal, comparable to authentic rS1-ADPr, appeared in the blot (Fig. 4a).

We applied this immunoblotting assay to investigate ADP-ribosylation and RNAylation *in vivo.* We expressed a plasmid-borne copy of rS1 in non-infected or T4-infected *E. coli*. Subsequently, rS1 was affinity-purified and its ADP-ribosylation analysed by pan-ADPr blotting (Extended Data Fig. 7b). In agreement with our mass-spectrometric data, this experiment revealed extensive ADP-ribosylation of rS1 only in the T4-infected sample. After nuclease P1-treatment, the pan-ADPr signal intensity of the rS1 band increased significantly (Fig. 4b), indicating that ~ 30 % of the modified rS1 was RNAylated *in vivo* (measured as the difference between P1-treated and nuclease untreated sample). Moreover, the signal for ADP-ribose disappeared upon ARH1 treatment, again confirming the nature of the RNA-protein linkage (Extended data Fig. 7b).

A recognition motif for ModB

How ModB identifies its targets remains a puzzle. Target protein rS1 contains oligonucleotide-binding (OB) domains [22]. One structural variant of OB folds is the S1 domain, present in rS1 in six copies that vary in sequence (Extended Data Fig. 8a,b). We speculated that the S1 domain might be important for substrate recognition by ModB. To characterise ModB's specificity for different rS1 domains, we individually cloned, expressed and purified each S1 domain of rS1 and applied them in our RNAylation assay (Fig. 4 c,d and Extended Data Fig. 8c,d). For rS1 domains D2 and D6 we determined high RNAylation signals. In comparison, rS1 D1, D3, D4 and D5 domains were modified to a much lesser extent. Alignment of D2 and D6 of rS1, and the S1 domain of PNPase, another protein in *E. coli* that possess an S1 domain, revealed that these S1 motifs share an arginine residue as part of the loop connecting strands 3 and 4 of the β-barrel [25] (Extended Data Fig. 8b). This loop is packed on the top of the β-barrel, thereby likely accessible for ModB. For rS1 D2, this particular residue is R139, which we had shown to be modified by mass spectrometry (Fig. 3f). Mutation analysis confirmed that the ADP-ribosylation level of D2 is dramatically reduced if R139 is substituted by alanine or lysine (Extended Data Fig. 9). Based on these findings, we screened for other *E. coli* proteins that harbour an S1 domain with an arginine in the loop between strands 3 and 4, and identified RNase E. In our *in vitro* assays, RNase E, which carries the S1 motif in its active site, was efficiently modified by ModB, while control proteins without S1 domain (BSA, NudC inactive quadruple mutant) were not, supporting the identification of the subgroup of S1 domains with an embedded arginine as the RNAylation target motif (Fig. 4e,f).

Modification and T4 replication cycle

rS1 is an important RNA-binding protein required for the translation of virtually all cellular mRNAs in *E. coli.* To investigate the biological consequences of rS1 modification by ModB, we analysed rS1 levels during T4 infection using an *E. coli* strain that contains a chromosomal fusion of rS1 with a FLAG-tag (Fig. 4g and Extended Data Fig. 10a). Immediately after infection, rS1 levels dropped steeply, whereas they increased moderately over 20 min in the absence of T4. We thus speculated that ADP-ribosylation and/or RNAylation might influence the stability of rS1. To test this hypothesis, we overexpressed human ARH1 in *E. coli* during T4 infection, thought to remove ADP-ribose and linked RNA. As a control, we overexpressed a largely inactive ARH1 D55,56A mutant. Indeed, with active ARH1, the ADP-ribosylation

signal was dramatically reduced (Extended Data Fig. 10b), while the mutant showed a pattern similar to the parent strain (Extended Data Fig. 10a). Using these constructed *E. coli* strains, we analysed the influence of ADP-ribosylation and RNAylation on rS1 levels during phage infection. Indeed, the strain expressing active ARH1 showed an increase in rS1 levels over time, like the uninfected sample, whereas the mutant strain exhibited declining levels, like the T4-infected sample without ARH1 (Extended Data Fig. 10b,c). Thus, the removal of ADPr and RNA chains during phage infection coincides with a stabilisation of the rS1 level.

To investigate if these modifications are important for the lysogenic behaviour of the phage, we infected *E. coli* strains expressing either ARH1 or its inactive mutant with T4 and monitored the optical density over time (Fig. 4i). In the inactive mutant strain, bacterial lysis started 50 min post-infection, while delayed lysis (120 min) was observed when active ARH1 was overexpressed (Fig. 4i). Collectively, these data indicate that ADP-ribosylation and/or RNAylation interfere with protein stability and modulate the course and efficiency of T4 infection.

Discussion

To date, all interactions between RNAs and proteins are described to be based on non-covalent interactions [26]. In contrast, we show here that ADP-ribosyltransferases can attach NAD-capped RNAs to target proteins in a covalent fashion. This finding represents a distinct biological function of the NAD-cap on RNAs in bacteria, namely activation of the RNA for enzymatic transfer to an acceptor protein. We discovered that RNAylation of target proteins, a novel post-translational protein modification, plays a role in the infection of the bacterium *E. coli* by bacteriophage T4. Our data indicate that T4 ART ModB modifies proteins that possess an S1 RNA binding domain. We identified specific arginine residues to be modified, thereby increasing molecular weight and negative charge of the target protein and undoubtedly causing major changes of the properties and functions of the modified proteins. The post-translational modification of crucial players in bacterial translation and transcription demonstrates the importance of the known ADP-ribosylation and the newly discovered RNAylation reaction for bacteriophage pathogenicity. Introduction of the human ADP ribosylhydrolase ARH1, which removes these modifications, into *E. coli*, caused a significant delay in bacterial lysis upon phage infection.

Why do phage ARTs attach RNAs to proteins involved in translation? One possibility may be that these RNAs help (e.g., by base pairing) to preferentially recruit mRNAs encoding for phage proteins to the ribosomes and thereby guarantee their biosynthesis. Likewise, the observation that RNase E, the major player in RNA turnover in *E. coli*, is RNAylated at its catalytic centre by ModB may suggest that the T4 phage, after reprogramming transcription by Alt and ModA, shuts down RNA degradation in the host to ensure a long half-life of phage mRNAs. We are working vigorously on methods for identifying the RNAs attached to target proteins, which will allow the elucidation of their biochemical mechanisms.

ARTs are known to occur not only in bacteriophages, and ADP-ribosylated proteins have been detected in hosts upon infections by various viruses, including influenza, corona, and HIV. In addition to viruses using

ARTs as weapons, the mammalian antiviral defence system applies host ARTs to inactivate viral proteins. Moreover, mammalian ARTs and poly-(ADP-ribose) polymerases (PARPs) are regulators of critical cellular pathways and are known to interact with RNA [27]. Thus, ARTs in different organisms might catalyse RNAylation reactions, and RNAylation may be a phenomenon of broad biological relevance.

Finally, RNAylation may be considered as both a post-translational protein modification and a post-transcriptional RNA modification. Our findings challenge the established views of how RNAs and proteins can interact with each other. The discovery of these new RNA-protein conjugates comes at a time when the structural and functional boundaries between the different classes of biopolymers become increasingly blurry [28,29].

Declarations

ACKNOWLEDGEMENTS

We thank N. Beumer, S. J. Keding, J. Koch, M. Raabe, and M. Tamerler for experimental assistance. This work was supported by the European Commission (ERC Advanced Grant 882789 RNACoenzyme to A.J.), M.S. was supported by the Studienstiftung des Deutschen Volkes. K.H. is supported by the Max Planck Society, Baden-Württemberg Stiftung and Carl-Zeiss-Stiftung. H.U. is supported by a grant of the Deutsche Forschungsgemeinschaft (DFG-SPP1935).

AUTHOR CONTRIBUTIONS

K.H. and A.J. designed the study. K.H., M.S., J.G., F.A.B. cloned, expressed, purified and analysed ARTs and their target proteins. K.H., A.W. and M.S. prepared samples for mass spectrometry. A.W., L.M.W. and H.U. developed an LC/MS/MS pipeline to study ADP-ribosylation/RNAylation and analysed the data. A.W. and K.H. performed MALDI-TOF experiments. K.H., H.U. and A.J. supervised the work. K.H. and A.J. wrote the first draft, and all authors contributed to reviewing, editing and providing additional text for the manuscript.

COMPETING INTERESTS

The authors declare no competing interests.

MATERIALS & CORRESPONDENCE

Supplementary Information is available for this paper.

The datasets generated during and/or analysed during the current study are available from the corresponding author on reasonable request.

Correspondence should be addressed to AJ and KH.

References

1. Cohen, M. S. & Chang, P. Insights into the biogenesis, function, and regulation of ADP-ribosylation. *Nat Chem Biol* **14**, 236–243, doi:10.1038/nchembio.2568 (2018).
2. Tiemann, B. *et al.* ModA and ModB, two ADP-ribosyltransferases encoded by bacteriophage T4: catalytic properties and mutation analysis. *J Bacteriol* **186**, 7262–7272, doi:10.1128/JB.186.21.7262-7272.2004 (2004).
3. Koch, T., Raudonikiene, A., Wilkens, K. & Rüger, W. Overexpression, purification, and characterisation of the ADP-ribosyltransferase (gpAlt) of bacteriophage T4: ADP-ribosylation of E. coli RNA polymerase modulates T4 "early" transcription. *Gene Expr* **4**, 253–264 (1995).
4. Cahova, H., Winz, M. L., Höfer, K., Nübel, G. & Jäschke, A. NAD captureSeq indicates NAD as a bacterial cap for a subset of regulatory RNAs. *Nature* **519**, 374–377, doi:10.1038/nature14020 (2015).
5. Jiao, X. *et al.* 5' End Nicotinamide Adenine Dinucleotide Cap in Human Cells Promotes RNA Decay through DXO-Mediated deNADding. *Cell* **168**, 1015–1027 e1010, doi:10.1016/j.cell.2017.02.019 (2017).
6. Chen, Y. G., Kowtoniuk, W. E., Agarwal, I., Shen, Y. & Liu, D. R. LC/MS analysis of cellular RNA reveals NAD-linked RNA. *Nat Chem Biol* **5**, 879–881, doi:10.1038/nchembio.235 (2009).
7. Fehr, A. R. *et al.* The impact of PARPs and ADP-ribosylation on inflammation and host-pathogen interactions. *Genes Dev* **34**, 341–359, doi:10.1101/gad.334425.119 (2020).
8. Simon, N. C., Aktories, K. & Barbieri, J. T. Novel bacterial ADP-ribosylating toxins: structure and function. *Nat Rev Microbiol* **12**, 599–611, doi:10.1038/nrmicro3310 (2014).
9. Luscher, B. *et al.* ADP-Ribosylation, a Multifaceted Post-translational Modification Involved in the Control of Cell Physiology in Health and Disease. *Chem Rev* **118**, 1092–1136, doi:10.1021/acs.chemrev.7b00122 (2018).
10. Morales-Filloy, H. G. *et al.* The 5' NAD Cap of RNAIII Modulates Toxin Production in Staphylococcus aureus Isolates. *J Bacteriol* **202**, doi:10.1128/JB.00591-19 (2020).
11. Frindert, J. *et al.* Identification, Biosynthesis, and Decapping of NAD-Capped RNAs in B. subtilis. *Cell Rep* **24**, 1890–1901 e1898, doi:10.1016/j.celrep.2018.07.047 (2018).
12. Walters, R. W. *et al.* Identification of NAD + capped mRNAs in Saccharomyces cerevisiae. *Proc Natl Acad Sci U S A* **114**, 480–485, doi:10.1073/pnas.1619369114 (2017).
13. Wang, Y. *et al.* NAD(+)-capped RNAs are widespread in the Arabidopsis transcriptome and can probably be translated. *Proc Natl Acad Sci U S A* **116**, 12094–12102, doi:10.1073/pnas.1903682116 (2019).
14. Zhang, Y. *et al.* Extensive 5'-surveillance guards against non-canonical NAD-caps of nuclear mRNAs in yeast. *Nat Commun* **11**, 5508, doi:10.1038/s41467-020-19326-3 (2020).
15. Höfer, K. & Jäschke, A. Epitranscriptomics: RNA Modifications in Bacteria and Archaea. *Microbiol Spectr* **6**, doi:10.1128/microbiolspec.RWR-0015-2017 (2018).

16. Miller, E. S. *et al.* Bacteriophage T4 genome. *Microbiol Mol Biol Rev* **67**, 86–156, table of contents, doi:10.1128/MMBR.67.1.86-156.2003 (2003).
17. Rohrer, H., Zillig, W. & Mailhammer, R. ADP-ribosylation of DNA-dependent RNA polymerase of Escherichia coli by an NAD+: protein ADP-ribosyltransferase from bacteriophage T4. *Eur J Biochem* **60**, 227–238, doi:10.1111/j.1432-1033.1975.tb20995.x (1975).
18. Depping, R., Lohaus, C., Meyer, H. E. & Ruger, W. The mono-ADP-ribosyltransferases Alt and ModB of bacteriophage T4: target proteins identified. *Biochem Bioph Res Co* **335**, 1217–1223, doi:10.1016/j.bbrc.2005.08.023 (2005).
19. Skorko, R., Zillig, W., Rohrer, H., Fujiki, H. & Mailhammer, R. Purification and properties of the NAD+: protein ADP-ribosyltransferase responsible for the T4-phage-induced modification of the alpha subunit of DNA-dependent RNA polymerase of Escherichia coli. *Eur J Biochem* **79**, 55–66, doi:10.1111/j.1432-1033.1977.tb11783.x (1977).
20. Tiemann, B., Depping, R. & Ruger, W. Overexpression, purification, and partial characterisation of ADP-ribosyltransferases modA and modB of bacteriophage T4. *Gene Expr* **8**, 187–196 (1999).
21. Höfer, K. *et al.* Structure and function of the bacterial decapping enzyme NudC. *Nat Chem Biol* **12**, 730–734, doi:10.1038/nchembio.2132 (2016).
22. Goelz, S. & Steitz, J. A. Escherichia coli ribosomal protein S1 recognises two sites in bacteriophage Qbeta RNA. *J Biol Chem* **252**, 5177–5179 (1977).
23. Cervantes-Laurean, D., Jacobson, E. L. & Jacobson, M. K. Glycation and glycoxidation of histones by ADP-ribose. *J Biol Chem* **271**, 10461–10469, doi:10.1074/jbc.271.18.10461 (1996).
24. Oka, S., Kato, J. & Moss, J. Identification and characterisation of a mammalian 39-kDa poly(ADP-ribose) glycohydrolase. *J Biol Chem* **281**, 705–713, doi:10.1074/jbc.M510290200 (2006).
25. Bycroft, M., Hubbard, T. J., Proctor, M., Freund, S. M. & Murzin, A. G. The solution structure of the S1 RNA binding domain: a member of an ancient nucleic acid-binding fold. *Cell* **88**, 235–242, doi:10.1016/s0092-8674(00)81844-9 (1997).
26. Hentze, M. W., Castello, A., Schwarzl, T. & Preiss, T. A brave new world of RNA-binding proteins. *Nat Rev Mol Cell Biol* **19**, 327–341, doi:10.1038/nrm.2017.130 (2018).
27. Ke, Y., Zhang, J., Lv, X., Zeng, X. & Ba, X. Novel insights into PARPs in gene expression: regulation of RNA metabolism. *Cell Mol Life Sci* **76**, 3283–3299, doi:10.1007/s00018-019-03120-6 (2019).
28. Otten, E. G. *et al.* Ubiquitylation of lipopolysaccharide by RNF213 during bacterial infection. *Nature*, doi:10.1038/s41586-021-03566-4 (2021).
29. Flynn, R. A. *et al.* Small RNAs are modified with N-glycans and displayed on the surface of living cells. *Cell*, doi:10.1016/j.cell.2021.04.023 (2021).
30. Tsuge, H. *et al.* Structural basis of actin recognition and arginine ADP-ribosylation by Clostridium perfringens iota-toxin. *Proc Natl Acad Sci U S A* **105**, 7399–7404, doi:10.1073/pnas.0801215105 (2008).

Methods

General

Reagents were purchased from Sigma-Aldrich and used without further purification. Oligonucleotides were purchased from Integrated DNA Technologies, Inc. DNA and RNA concentrations were determined by measurements with the NanoDrop ND-1000 spectrophotometer. Radioactively labelled proteins or nucleic acids were visualised using storage phosphor screens (GE Healthcare) and a Typhoon 9400 imager (GE Healthcare).

Preparation of 5'PPP-/5'P-/5'-NAD-RNA by in vitro transcription

DNA template for Qβ-RNA was amplified by PCR. PCR products were analysed by 1 % agarose gel electrophoresis and purified using the QIAquick PCR purification kit (QIAGEN). 5'-triphosphate (PPP) Qβ-RNA was synthesized by *in vitro* transcription (IVT) in the presence of 1x transcription buffer (40 mM Tris, pH 8.1, 1 mM spermidine, 10 mM $MgCl_2$, 0.01 % Triton-X-100), 5 % DMSO, 10 mM DTT, 4 mM of each NTP, 20 µg of T7 RNA polymerase (2 mg/ml) and 200 nM DNA template. The same conditions were applied for the synthesis of a mixture of α-^{32}P-labelled 5'-NAD- and PPP-Qβ-RNAs except for the presence of 2 mM ATP, 80 µCi ^{32}P-α-ATP and 4 mM NAD instead of 4 mM ATP. The IVT reactions were incubated at 37°C for 4 h and digested with DNase I (Roche). RNA was purified by denaturing PAGE and isopropanol-precipitation, and resuspended in Millipore water. RNA sequences are listed in Extended Data Table 1.

To convert 5'-PPP-RNAs into 5'-monophosphate RNAs (5'-P-RNAs), 250 pmol of Qβ-RNA were treated with 60 U of RNA 5'-polyphosphatase (Epicentre) in 1x polyphosphatase reaction buffer at 37°C for 70 min. Protein was removed from 5'-P-RNAs by phenol-chloroform extraction and residual phenol-chloroform removed by three rounds of diethyl ether extraction. 5'-P-RNAs were isopropanol precipitated and dissolved in Millipore water.

5'-radiolabelling of 5'-monophosphate and NAD-capped RNAs

120 pmol of 5'-P-Qβ-RNA, or 6.25 nmol of 5'-P-RNA 8-mer were treated with 50 U of T4 polynucleotide kinase (PNK) in 1x reaction buffer B and 1,250 µCi ^{32}P-γ-ATP. The reaction was incubated at 37°C for 2 h. The resulting 5'-^{32}P-RNA 8-mer/ 5'-^{32}P-Qβ-RNA were separated from residual protein by phenol-chloroform extraction. The remaining ^{32}P-γ-ATP was removed by washing with 3 column volumes of Millipore water and centrifugation in 10 kDa (Qβ-RNA) or 3 kDa (8-mer) Amicon filters (Merck Millipore) at 14,000 rpm at 4°C for four times. RNA sequences are listed in Extended Data Table 1. To convert the purified 5'-^{32}P-RNAs into 5´-^{32}P-NAD-capped RNAs, 800 pmol of 5´-^{32}P-RNA 8-mer or 30 pmol of 5'-^{32}P-Qβ-RNA were each incubated in 50 mM $MgCl_2$ in the presence of a spatula tip of nicotinamide mononucleotide phosphorimidazolide (Im-NMN), synthesised as described in [1], at 50°C for 2 hours. RNAs were purified by washing with Millipore water and centrifugation in 10 kDa (Qβ-RNAs) or 3 kDa (8-mer) Amicon filters at 14,000 rpm at 4°C for four times. Concentrations of the 5'-^{32}P-RNAs were measured on the NanoDrop and

used to calculate the approximate concentrations of yielded 5′-NAD-capped ^{32}P-RNAs assuming an approximate yield of the imidazolide reaction of 50 % [1]. 5′-^{32}P-ADP-ribose-RNA 8mer (ADPr-8mer) was synthesised by incubation of 4.8 µM 5′-^{32}P-NAD-RNA 8mer and 0.08 µM ADP-ribosylcyclase CD38 in 1x degradation buffer at 37°C for 4 h. The reaction was purified by P/C/I-diethylether-extraction and filtration through 3 kDa filters washing with 4 column volumes of Millipore water.

Cloning of ADP-ribosyltransferases, ADP-ribose hydrolases and target proteins

To amplify bacteriophage T4 genes *modA*, *modB* and *alt*, a single plaque from T4 bacteriophage revitalisation was resuspended in Millipore water and used in a “plaque”-PCR, analogous to bacterial colony PCR. The gene encoding for the ADP-ribosylhydrolase ARH1 was purchased from IDT as gblocks and amplified by PCR. *E. coli* genes coding for rS1 and PNPase were PCR-amplified from genomic DNA of *E. coli* K12, which was isolated via GenElute Bacterial Genomic DNA Kit (Sigma-Aldrich). Nucleotide sequences are listed in Extended Data Table 2. XhoI and NcoI restriction sites were introduced during amplification using appropriate primers (Extended Data Table 3). The resulting PCR product was digested with XhoI and NcoI and cloned into pET-28c vector (Merck Millipore). After Sanger sequencing, the resulting plasmids were transformed into *E. coli* One Shot BL21 (DE3) (Life Technologies). The ARH1 D55,56A and rS1 mutants were generated by site-directed mutagenesis using a procedure based on the Phusion Site-Directed Mutagenesis Kit (Thermo Scientific). The resulting plasmids were sequenced and transformed into *E. coli* One Shot BL21 (DE3).

AHR1, ARH1 D55A D56A and rS1 were transferred from pET28 to pTAC-vector using specific primers with restriction sites for XhoI and SphI (Extended Data Table 3). The resulting PCR product was digested with XhoI and SphI and cloned into pTAC-MAT-2 (Sigma-Aldrich). The resulting plasmids were transformed into *E. coli* strain B and *E. coli* Ced64 (kind gift from Gerhart E. Wagner, Uppsala University). All strains used and generated in this work are summarised in Extended Data Table 4

Purification of rS1 domains and variants, PNPase Domain, RNase E (1-529), Alt, NudC V157A, E174A, E177A, E178A

IPTG-induced *E. coli* One Shot BL21 (DE3) containing the respective plasmid were cultured in LB medium at 37°C. Protein expression was induced at OD_{600} = 0.8, bacteria were harvested by centrifugation after 3 hours at 37°C and lysed by sonication (30 s, 50 % power, five times) in HisTrap buffer A (50 mM Tris-HCl pH 7.8, 1 M NaCl, 1 M Urea, 5 mM $MgSO_4$, 5 mM β-mercaptoethanol, 5 % glycerol, 5 mM imidazole, 1 tablet per 500 ml complete EDTA-free protease inhibitor cocktail (Roche)). The lysate was clarified by centrifugation (37,500 g, 30 min, 4°C) and the supernatant was applied to a 1 mL Ni-NTA HisTrap column (GE Healthcare). The protein was eluted with an imidazole gradient using an analogous gradient of HisTrap buffer B (HisTrap buffer A with 500 mM imidazole) and analysed by SDS–PAGE.

Further protein purification was achieved by size exclusion chromatography (SEC) through a Superdex™ 200 10/300 GL column (GE Healthcare) using a buffer containing 0.5 M NaCl and 25 mM Tris-HCl, pH 8.

Fractions of interest were analysed by SDS–PAGE, pooled and concentrated in Amicon Ultra-4 centrifugal filters (MWCO 10 kDa, centrifugation at 2,000 rpm., 4°C). Protein concentration was measured with the NanoDrop ND-1000 Spectrophotometer. Proteins were finally stored in buffer supplemented with 50 % glycerol at -20°C.

Purification of ARH1 and ARH1 D55,56A

E. coli BL21 DE3 pET28-ARH1 and BL21-pET28-ARH1 D55A D56A were grown to an OD_{600} = 0.6 at 37°C, 175 rpm. Afterwards, bacteria were allowed to cool to room temperature for 30 minutes. Expression was induced with 1 mM IPTG, and bacteria were finally grown overnight at room temperature, 175 rpm. Bacteria were harvested by centrifugation, and proteins were purified analogously to rS1 variants.

Purification of ModA

E. coli BL21 DE3 pET28-ModV were grown to an OD_{600} = 1 at 37°C, 175 rpm. Proteiexprssion was induced with 0.5 mM IPTG and bacteria were harvested by centrifugation after 3 hours at 37°C. Pelleted bacteria were resuspended in 50 mM NaH_2PO_4, pH 8, 300 mM NaCl, 1 mM DTT, 1 tablet per 500 ml complete EDTA-free protease inhibitor cocktail (Roche))and lysed by sonication (3 x 1 min, 50 % power). Lysates were centrifuged at 3,000 *g*, 4°C for 20 min. Sediments were washed by resuspension in 30 mL 50 mM Tris-HCl, pH 7.5, 2 mM EDTA, 100 mM NaCl, 1 M urea, 1 mM DTT, 1 tablet EDTA-free protease inhibitor (Roche), and centrifuged at 10,000 *g*, 4°C for 20 min. Pellets, containing inclusion bodies, were resuspended in 40 mL 100 mM Tris pH 11.6, 8 M urea, transferred to 12–14 kDa MWCO dialysis bags (Roth), and dialysed overnight against 50 mM NaH_2PO_4, 300 mM NaCl. Protein solutions were centrifuged at 20,000 *g*, 4°C for 30 min. Supernatants were batch-purified using disposable 10 mL columns (Thermo Fisher Scientific) packed with 2 mL Ni-NTA agarose (Jena Bioscience), and equilibrated with 10 column volumes (CV) of 50 mM NaH_2PO_4 (pH 8), 300 mM NaCl. Proteins were purified by washing the columns with 30 CV 50 mM NaH_2PO_4, 300 mM NaCl, 15 mM imidazole, eluted with 5 mL 50 mM NaH_2PO_4, 300 mM NaCl, 300 mM imidazole, and concentrated in Amicon Ultra-4 centrifugal filters (MWCO 10 kDa, centrifugation at 2,000 rpm, 4°C). Proteins were finally purified by SEC as described for rS1.

Purification of ModB

E. coli BL21 DE3 pET28-ModB were grown to an OD_{600} = 2.0 at 37°C, 185 rpm and cooled down to 4°C while shaking at 160 rpm for at least 30 min. Protein expression was induced by the addition of 1 mM IPTG. The cultures were then incubated for 120 min at 4°C, 160 rpm and bacteria harvested by centrifugation (4,000 rpm, 4°C, 25 min). The ModB protein was purified from the supernatant as described for rS1 variants.

In vitro ADP-ribosylation and RNAylation of protein rS1 with ^{32}P-labelled NAD, NAD-8mer and NAD-Qβ-RNA

0.3 µM protein rS1 were ADP-ribosylated in the presence of 0.25 µCi/µl ^{32}P-NAD or RNAylated in the presence of either 0.6 µM ^{32}P-NAD-8mer or 0.03 µM ^{32}P-NAD-Qβ-RNA by 1.4 µM ModB and in 1x transferase buffer (10 mM Mg(OAc)2, 22 mM NH4Cl, 50 mM Tris-acetate pH 7.5, 1 mM EDTA, 10 mM β-mercaptoethanol, 1 % glycerol) at 15°C for at least 120 minutes. 5 µL samples were taken after 0 (before addition of ModB), 1, 2, 5, 10, 30, 60 and 120 minutes and mixed with 5 µL 2x Laemmli buffer to stop the reaction. Reactions were assessed by 12 % SDS-PAGE and gels stained in Instant Blue solution (Sigma-Aldrich) for 10 min. Radioactive signals were visualised using storage phosphor screens (GE Healthcare) and a Typhoon 9400 imager (GE Healthcare). Intensities of radioactive bands were quantified using ImageQuant 5.2.

Kinetics of RNAylation in the presence of high NAD concentrations

Kinetic experiments for RNAylation in the presence of different NAD concentrations were performed using conditions for RNAylation and ADP-ribosylation as mentioned above. The kinetics were performed in 0.15 µM ^{32}P-NAD-RNA 8-mer with either 0.125 µM, 12.5 µM, 125 µM or 1.25 mM NAD corresponding to an approximate molar excess of NAD over ^{32}P-NAD-RNA 8-mer of 1-, 100-, 1,000- and 10,000-fold. The reactions temperatures were pre-adjusted to 15°C. 5 µL samples were taken after 0 (before addition of ModB), 1, 5, 10, 30, 60 and 120 minutes and mixed with 5 µl 2x Laemmli buffer to stop the reaction. Samples were analysed by 12 % SDS-PAGE analysis. 10 µL of a reference in 1x Laemmli buffer were applied to each SDS-polyacrylamide gel containing 1.91 pmol of protein rS1 modified by 6.74 pmol ModB in 1x transferase buffer and 0.15 µM ^{32}P-NAD-RNA 8-mer. Intensities of radioactive bands were quantified using ImageQuant 5.2. Relative RNAylation values were computed by the division of the individual intensity values by the intensity of the reference.

Investigation of self-RNAylation of ribosomal protein rS1

In scales of 20 µL reactions, 3.6 µM of ^{32}P-ADPr-8mer were either incubated with 2.6 µM of protein rS1, 3.9 µM of ModB or both 2.59 µM of protein rS1 and 3.89 µM of ModB in 1x transferase buffer. As a positive control, equal amounts of protein rS1 and ModB were incubated with 0.6 µM of ^{32}P-NAD-8mer. All reactions were incubated at 15°C for 60 minutes. Samples were taken before the addition of ModB (0 minutes), after 60 minutes of incubation and stopped by the addition of 1 volume 2x Laemmli buffer each. The reactions were analysed by 12 % SDS-PAGE and autoradiography imaging.

RNAylation of protein rS1 with Qβ-RNA and specificity for the 5'-NAD-cap

0.05 µM ^{32}P-NAD-Qβ-RNA, 0.15 µM 5'-^{32}P-Qβ-RNA or 0.15 µM 5'-^{32}PPP-Qβ-RNA were incubated with 2.3 µM of protein rS1 and 1.4 µM of ModB each in the presence of 1x transferase buffer at 15°C for 60 minutes. Samples were taken before the addition of ModB (0 minutes) and after 60 minutes of incubation and reactions stopped by the addition of 1 volume 2x Laemmli buffer. Reactions were analysed by 10 % SDS-PAGE applying a reference of rS1-ADPr (^{32}P) in 1x Laemmli buffer and autoradiography imaging.

Preparation of RNAylated and ADP-ribosylated rS1 for enzymatic treatments

ADP-ribosylation or RNAylation reactions performed with radio-labelled substrates were washed and equilibrated in 1x transferase or 1x degradation buffer for further enzymatic treatment. Therefore, the reactions were washed with 4 column volumes of the corresponding buffer via centrifugation at 10,000 x g, 4°C in 10 kDa Amicon filters.

Nuclease P1 digest of protein rS1 RNAylated with Qβ-RNA (rS1-Qβ-RNA)

19 µL of rS1/rS1-Qβ-RNA (^{32}P) mixture equilibrated in 1x transferase buffer were incubated with either 1 µL of nuclease P1 or 1 µL of Millipore water at 37°C for 60 minutes. Samples were taken before the addition of enzyme (0 minutes) and after 60 minutes of incubation and reactions stopped by addition of 1 volume 2x Laemmli buffer. Reactions were analysed by 10 % SDS-PAGE using rS1-ADPr (^{32}P) as a reference and autoradiography imaging.

Digest of rS1-8mer and rS1-ADPr by NudC and alkaline phosphatase

28 µL of rS1/rS1-8mer (^{32}P) mixture or rS1/rS1-ADPr (^{32}P) mixture equilibrated in 1x degradation buffer (12.5 mM Tris-HCl, pH 7.5, 25 mM NaCl, 25 mM KCl, 5 mM $MgCl_2$) were either incubated with 2.3 µM of NudC and 1 U of alkaline phosphatase (FastAP, Thermo Scientific) or 2 µL of Millipore water as a negative control at 37°C. Samples were taken before the addition of enzymes/Millipore water and after 60 minutes of incubation. Reactions were stopped by adding 1 volume 2x Laemmli buffer, and additional samples were taken and resuspended in 1 volume 2x PAGE Loading Dye. Samples were analysed by either 12 % SDS- or denaturing 20 % PAGE using ^{32}P-NAD-8mer and 5'-^{32}P-8mer as references. Autoradiography imaging was applied to all analyses.

Tryptic digest of rS1-8mer and rS1-ADPr

19 µL of both rS1/rS1-8mer (^{32}P) mixture and rS1/rS1-ADPr (^{32}P) mixture in 1x degradation buffer were incubated with either 0.2 µg Trypsin (Sigma, EMS0004, mass spectrometry grade) or Millipore water as a negative control at 37°C. Samples were taken before the addition of Trypsin/Millipore water (0 minutes) and after 120 minutes of incubation. Reactions were stopped by adding 1 volume 2x Laemmli buffer to samples and were analysed by 12 % SDS-PAGE and autoradiography imaging.

Chemical removal of ADP-Ribosylation and RNAylation in vitro

Aliquots from washed and equilibrated ADP-ribosylated (1 µL) and RNAylated (2 µL) (^{32}P) rS1 were treated with either 10 mM $HgCl_2$ or 500 mM NH_2OH [2,3] at 37°C for 1h. Enzymatic reactions were stopped by addition of 2x Laemmli-Buffer and analysed by 12 % SDS-PAGE.

Enzymatic removal of ADP-Ribosylation and RNAylation in vitro

Aliquots from washed and equilibrated ADP-ribosylated (1 µL) and RNAylated (2 µL) rS1 (^{32}P) were treated with 0.5 U endonuclease P1 (Sigma-Aldrich) [4] or 0.95 µM ARH1 or ARH3 (human, recombinant, Enzo Life Science) [5] in the presence of 10 mM $Mg(OAc)_2$, 22 mM NH_4Cl, 50 mM HEPES, 1 mM EDTA, 10 mM β-mercaptoethanol and 1 % (v/v) glycerol in a total volume of 20 µL at 37°C for 1 h. Enzymatic reactions were stopped by the addition of 2x Laemmli-Buffer and analysed by 12 % SDS-PAGE.

Inhibition of RNAylation and ADP-ribosylation with 3-methoxybenzamide

20 µL reactions of 1.4 µM ModB and 2.3 µM protein rS1 with either 1 µM of ^{32}P-NAD-8mer or 3 µM 5'-^{32}P-8mer were incubated in the presence of 2 mM 3-methoxybenzamide (50 mM stock in DMSO) or in the absence of the inhibitor (DMSO only) at 15°C [6]. Samples were taken before the addition of ModB (0 minutes) and after 60 minutes of incubation with ModB. Reactions were stopped by the addition of 1 volume 2x Laemmli buffer and analysed by 12 % SDS-PAGE.

Cultivation of E. coli B strain and T4 phage infection

Pre-cultures of *E. coli* B strain pTAC-rS1 were incubated in LB medium with 100 µg/mL ampicillin at 37°C, 185 rpm overnight. For main cultures, 150 mL LB medium with 100 µg/mL ampicillin were inoculated with pre-culture to an OD_{600} = 0.1. At OD_{600} = 0.4 protein expression was induced by the addition of 1 mM IPTG. At an OD_{600} = 0.8, cultures were either infected with bacteriophage T4 at an MOI 10 (20 mL phage solution) (DSM 4505, Leibniz Institute DSMZ). For the negative control, 20 mL LB medium were added to the culture. Cultures were incubated for 20 min at 37°C, 240 rpm. Bacteria were harvested by centrifugation at 4,000 x g at room temperature for 15 min. Pellets were stored at -80°C.

Purification of His-tagged rS1 from infected E. coli strain B pTAC-rS1

Bacterial pellets were resuspended in 10 mL buffer A and lysed via sonication (1 x 5 min, cycle 2, 50 % power). Lysates were centrifuged at 37,500 g, 4°C for 30 min. The supernatant was filtered through 0.45 µm filters. rS1 from bacteriophage T4-infected or non-infected *E. coli* B strain was purified from the supernatant by gravity Ni-NTA affinity chromatography. 1 mL of Ni-NTA agarose slurry was added to a 10 mL propylene column and equilibrated in buffer A. The supernatant was loaded onto the column twice. The column was washed with a mixture of 95 % buffer A and 5 % buffer B containing 29.75 mM imidazole. Protein was eluted from the column with 10 mL buffer B.

His-tagged-protein rS1 from T4-infected or uninfected *E. coli* B strain pTAC-rS1 was washed with two filter volumes of 1x degradation buffer (12.5 mM Tris-HCl, pH 7.5, 25 mM NaCl, 25 mM KCl, 5 mM $MgCl_2$) by centrifugation in 10 kDa Amicon Ultra-4 centrifugal filters at 5,000 g, 4°C and concentrated to a final volume of 120 µL. The fractions were analysed by 12 % SDS-PAGE analysis, and the gel was stained in Instant Blue solution for 10 min and imaged immediately.

Purification of endogenous rS1 from infected E. coli strain B

For isolation of endogenous protein rS1, ribosomes were first isolated as described in [7]. Bacterial pellets of T4 infected and non-infected *E. coli* B strain were resuspended in resuspension buffer (20 mM $MgCl_2$, 200 mM NH_4Cl, 20 mM Tris-HCl pH 7.5, 0.1 mM EDTA, 6 mM β-mercaptoethanol) and cells were lysed by sonication. The lysate was cleared by ultracentrifugation at 30,000 x g, 4°C, 30 min. 15 mL of cleared supernatant were loaded onto 1 volume sucrose cushion (20 mM $MgCl_2$, 200 mM NH_4Cl, 20 mM Tris-HCl pH 7.5, 0.1 mM EDTA, 6 mM β-mercaptoethanol, 30 % (w/v) sucrose) in glass ultracentrifuge tubes, which were centrifuged at 67,000 x g, 18°C for 24 hours. The supernatant was discarded, the ribosomal pellets washed with rS1 wash buffer (20 mM $Mg(OAc)_2$, 1 M NH_4Cl, 10 mM Tris-HCl pH 7.6, 7 mM β-mercaptoethanol) carefully and resuspended in 4 mL of rS1 wash buffer.

Endogenous rS1 was then purified from resuspended ribosomes using self-synthesised poly(U)-Sepharose [8]. Synthesis of poly(U)-Sepharose was performed according to [9] with slight modifications. 700 mg of cyan bromide-activated Sepharose beads were resuspended in 30 mL 0.1 M NaCl, 2 mM Tris-HCl pH 7.5 and incubated at 4°C for 2 hours under rotation. Beads were pelleted by centrifugation at 15,567 x g for 3 minutes and the supernatant removed. Beads were then resuspended in 30 mL of 0.2 M 4-morpholine-ethanesulfonic acid (MES) and pelleted again to discard the supernatant. For coupling of poly-uridine (poly(U)) material to the beads, 10 mg of poly(U) material (Santa Cruz) resuspended in 5 mL of 0.2 M MES pH 6.0 were added to the equilibrated, activated Sepharose beads and the suspension incubated at 4°C overnight. The resulting poly(U)-Sepharose was equilibrated in rS1 wash buffer by washing with 4 polypropylene column volumes (10 mL). 6 mL of poly(U)-Sepharose suspension were obtained for isolation of endogenous rS1 from ribosomes. To specifically isolate rS1, 3 mL of the beads were mixed with 4 mL of the isolated ribosomes and incubated at 4°C for 30 minutes. The bead-protein mixture was subjected to gravity affinity purification with 10 mL polypropylene columns. Ribosomes were washed with 4 column volumes of rS1 wash buffer and endogenous rS1 eluted with 10 mL rS1 elution buffer (20 mM $Mg(OAc)_2$, 1 M NH_4Cl, 10 mM Tris-HCl pH 7.6, 7 mM β-mercaptoethanol, 7 M urea). Afterwards, beads were re-equilibrated in rS1 wash buffer and the washing and elution steps were repeated once. Eluates of the same sample were pooled, concentrated and analysed by SDS-PAGE.

LC-MS/MS

To identify ADPr-modification sites on rS1, 100 µg of *in vitro* or *in vivo* modified-rS1 were digested with trypsin (sequencing grade modified, Promega) overnight at a 1:20 (w/w) ratio at 37°C. The digest was stopped by adding 0.5 % trifluoroacetic acid and 5 % acetonitrile (v/v), followed by desalting using acommercially available pre-packed C18 column for acidic RP C18 desalting (Harvard Apparatus, Microspin C18 Column) and enriched using TiO_2 as described elsewhere for protein-RNA cross-link enrichment [10]. Next, the sample was subjected to LC-MS analysis using a Dionex UltiMate 3000 UHPLC$^+$ focused system (Thermo Scientific) with a C18 analytical column (75 µm × 300 mm, ReproSil-Pur 120 C18-AQ, 1.9 µm, Dr. Maisch GmbH, packed in house). Peptides were separated by RP C18 chromatography on a 58 min multi-step gradient (flow rate 0.3–0.4 µl min^{-1}). Eluting peptides were analysed with an orbritrap mass spectrometer (QExactive HF-X or Orbitrap Lumos Fusion, Thermo

Scientific) with the following settings: MS1 spectra in profile mode (resolution of 120k), MS2 spectra in centroid mode (resolution of 30k); isolation window set to 1.6 *m/z* and dynamic exclusion set to 7 s. Raw data were searched in an open search using PD2.2 (SEQUEST search engine) to identify possible adduct masses that could correspond to RNA or NAD. Precursor mass tolerance was set to 700 Da and fragment mass tolerance was set to 0.02 Da. We only identified ribose-5-phosphate as a shorter peptide modification reliably with an adduct mass of mz = 212.0086 and validated results in stringent searches with precursor mass tolerance set to 7 ppm and fragment mass tolerance set to 10 ppm. Identified peptides were filtered on PSM level to an FDR of 1 %.

MALDI-TOF

To identify larger adduct masses than ribose-5-phosphate that escaped LC-MS detection, we performed MALDI-TOF experiments. Modified rS1 peptides were prepared as described above at basic pH. Formic acid was substituted with 10 mM ammonium hydroxide in all RP-C18 buffers. Eluted sample was mixed with 2,5-dihydroxy benzoic acid (DHB) and then spotted onto an MTP stainless steel plate in a double layer fashion. MS data was acquired on a Bruker Autoflex Speed MALDI-TOF instrument in positive reflectron mode for survey scans or LIFT mode for pseudo MS2. The instrument was calibrated against BSA peptides and then recalibrated against wt rS1 peptides to 20 ppm mass error. Record spectra were baseline corrected but not smoothened.

Western Blotting

Proteins were separated by 10 % SDS-PAGE and gels were equilibrated in transfer buffer (25 mM Tris, pH 8.3, 192 mM glycine, 20 % [v/v] methanol). 0.2 µm polyvinylidene difluoride (PVDF) membranes (GE Healthcare) were activated in methanol for 1 min and equilibrated in transfer buffer. Proteins were transferred from gels to PVDF membranes in a semi-dry manner at 300 mA for 1.5 h, if not indicated differently. After the transfer, membranes were dehydrated by soaking in methanol and washed 2x with TBS-Tween (TBS-T; 10 mM Tris-HCl, pH 7.5, 150 mM NaCl, 0.05 % [v/v] Tween® 20). Afterwards 10 mL blocking buffer (5 % [w/v] milk powder in TBS-T) were added to the membranes and incubated at room temperature for 1 h. In order to detect ADP-ribosylated proteins, membranes were incubated with 0.1 ng/mL primary antibody MABE1016 (Merck) in 10 mL washing buffer (1 % [w/v] milk powder in TBS-T) at 4°C overnight [11]. Membranes were washed and incubated with 10 mL of a 1:10,000 dilution of the horseradish-peroxidase-(HRP)-goat-anti-rabbit-IgG secondary antibody (Advansta) in washing buffer at room temperature for 1 h. Afterwards, membranes were washed with PBS. Proteins with detected modifications were visualised by chemiluminescence using the SignalFire ECL Reagent or the SignalFire Elite ECL Reagent (Cell Signaling Technology) according to the manufacturer's instructions.

If proteins in SDS-PAGE gels needed to be visualised before blotting, a 2,2,2-trichloroethanol (TCE) staining method [12] was used. Resolving gels were supplemented with 0.5 % (v/v) TCE. For visualisation, gels were activated by ultraviolet transillumination (300 nm) for 60 s. Proteins then showed fluorescence in the visible spectrum.

Quantification of RNAylation

rS1 proteins were isolated from *E. coli* strain B pTAC rS1 infected or non-infected with bacteriophage T4. 1.5 µM rS1 were digested with 1 µM ARH1 in the presence of 12.5 mM Tris-HCl pH 7.5, 25 mM NaCl, 25 mM KCl and 5 mM $MgCl_2$. 1.5 µM rS1 were digested with 0.5 U endonuclease P1 in 100 mM $Mg(OAc)_2$, 220 mM NH_4Cl, 500 mM HEPES pH 7.5, 10 mM EDTA, 100 mM β-mercaptoethanol and 10 % glycerol. Digests were incubated at 37°C for 2 hours. Afterwards, digests were ethanol-precipitated by the addition of 9 volumes of ethanol and precipitated by centrifugation (14,000 rpm) at 4°C for 1 h. Protein pellets were resuspended in 10 µL 1x Laemmli buffer and analysed via Western blot. ADPr-modifications were detected by the primary antibody MABE1016 (Merck) as described above.

Reprobing of PVDF membranes with sodium azide

Following the visualisation of the chemiluminescence signal, the PVDF membranes were washed with Dulbecco's PBS. Subsequently, the membranes were incubated in blocking solution (5 % [w/v] milk powder in TBS-T) with 1 mM sodium azide for 3 hours at 4°C. Afterwards, the membranes were washed in TBS-T 6 times, for 5 minutes each. Inactivation of HRP was visualised by chemiluminescence using the SignalFireTM ECL Reagent or the SignalFireTM Elite ECL Reagent.

Detection of the FLAG-tagged rS1

PVDF membranes were incubated with a 1:10,000 dilution of the anti-FLAG-M2 antibody (Thermo Fisher Scientific) in a washing solution at 4°C overnight. The membranes were washed 3 times with washing solution and incubated in a 1:10,000 dilution of the HRP-goat-anti-mouse-IgG (Advansta) for 1 h at room temperature. FLAG-tagged rS1 was visualised by chemiluminescence as described above.

T4 Phage infection of E. coli strain B and Ced64 with $ARH1^{WT}$ and $ARH^{D55,56A}$ plasmids

E. coli B strain or *E. coli* Ced64 containing the plasmid pTAC $ARH1^{WT}$ or pTAC $ARH1^{D55,56A}$ were inoculated in 40 mL LB medium supplemented with 100 µg/mL ampicillin at OD_{600} = ~ 0.1 and incubated at room temperature, 150 rpm. At OD_{600} = 0.3, the expression of $ARH1^{WT}$ or $ARH1^{D55,56A}$ was induced with 1 mM IPTG. At OD_{600} = 0.8, cultures were infected with T4 at a MOI 10. After 0, 5, 10, 30, 60, 90, 110, 140 and 200 minutes, the OD_{600} values of the cultures were measured. At the indicated time points, 100 µL aliquots were taken, and bacteriophage T4 infections stopped by the addition of 2x Laemmli buffer. The aliquots were analysed via Western Blotting.

Visualisation of $ARH1^{WT}$ and $ARH1^{D55,56A}$ via Western Blotting

The proteins were transferred onto a PVDF membrane as described above. Following the exact same treatment, the membranes were incubated in a 1:2,000 dilution of 6x-His Tag Monoclonal Antibody (HIS.H8) in 10 mL of washing solution. The following day, horseradish-peroxidase-(HRP)-goat-anti-

mouse-IgG (Advansta, San Jose, USA) was used as a secondary antibody. His-tagged proteins were visualised by chemiluminescence as described above.

REFERENCES

1 Höfer, K., Abele, F., Schlotthauer, J. & Jäschke, A. Synthesis of 5'-NAD-Capped RNA. *Bioconjug Chem* **27**, 874–877, doi:10.1021/acs.bioconjchem.6b00072 (2016).

2 Hsia, J. A. *et al.* Amino acid-specific ADP-ribosylation. Sensitivity to hydroxylamine of [cysteine(ADP-ribose)]protein and [arginine(ADP-ribose)]protein linkages. *J Biol Chem* **260**, 16187–16191 (1985).

3 McDonald, L. J., Wainschel, L. A., Oppenheimer, N. J. & Moss, J. Amino acid-specific ADP-ribosylation: structural characterisation and chemical differentiation of ADP-ribose-cysteine adducts formed nonenzymatically and in a pertussis toxin-catalysed reaction. *Biochemistry-Us* **31**, 11881–11887, doi:10.1021/bi00162a029 (1992).

4 Silberklang, M., Gillum, A. M. & RajBhandary, U. L. The use of nuclease P1 in sequence analysis of end group labeled RNA. *Nucleic Acids Res* **4**, 4091–4108, doi:10.1093/nar/4.12.4091 (1977).

5 Abplanalp, J. *et al.* Proteomic analyses identify ARH3 as a serine mono-ADP-ribosylhydrolase. *Nat Commun* **8**, 2055, doi:10.1038/s41467-017-02253-1 (2017).

6 Banasik, M., Komura, H., Shimoyama, M. & Ueda, K. Specific inhibitors of poly(ADP-ribose) synthetase and mono(ADP-ribosyl)transferase. *J Biol Chem* **267**, 1569–1575 (1992).

7 Romilly, C., Deindl, S. & Wagner, E. G. H. The ribosomal protein S1-dependent standby site in tisB mRNA consists of a single-stranded region and a 5' structure element. *Proc Natl Acad Sci U S A* **116**, 15901–15906, doi:10.1073/pnas.1904309116 (2019).

8 Subramanian, A. R., Rienhardt, P., Kimura, M. & Suryanarayana, T. Fragments of ribosomal protein S1 and its mutant form m1-S1. Localisation of nucleic-acid-binding domain in the middle region of S1. *Eur J Biochem* **119**, 245–249, doi:10.1111/j.1432-1033.1981.tb05600.x (1981).

9 Wagner, A. F., Bugianesi, R. L. & Shen, T. Y. Preparation of sepharose-bound poly (rI:rC). *Biochem Biophys Res Commun* **45**, 184–189, doi:10.1016/0006-291x(71)90067-2 (1971).

10 Sonnleitner, E. *et al.* Interplay between the catabolite repression control protein Crc, Hfq and RNA in Hfq-dependent translational regulation in Pseudomonas aeruginosa. *Nucleic Acids Res* **46**, 1470–1485, doi:10.1093/nar/gkx1245 (2018).

11 Gibson, B. A., Conrad, L. B., Huang, D. & Kraus, W. L. Generation and Characterization of Recombinant Antibody-like ADP-Ribose Binding Proteins. *Biochemistry-Us* **56**, 6305–6316, doi:10.1021/acs.biochem.7b00670 (2017).

12 Ladner, C. L., Yang, J., Turner, R. J. & Edwards, R. A. Visible fluorescent detection of proteins in polyacrylamide gels without staining. *Anal Biochem* **326**, 13–20, doi:10.1016/j.ab.2003.10.047 (2004).

Figures

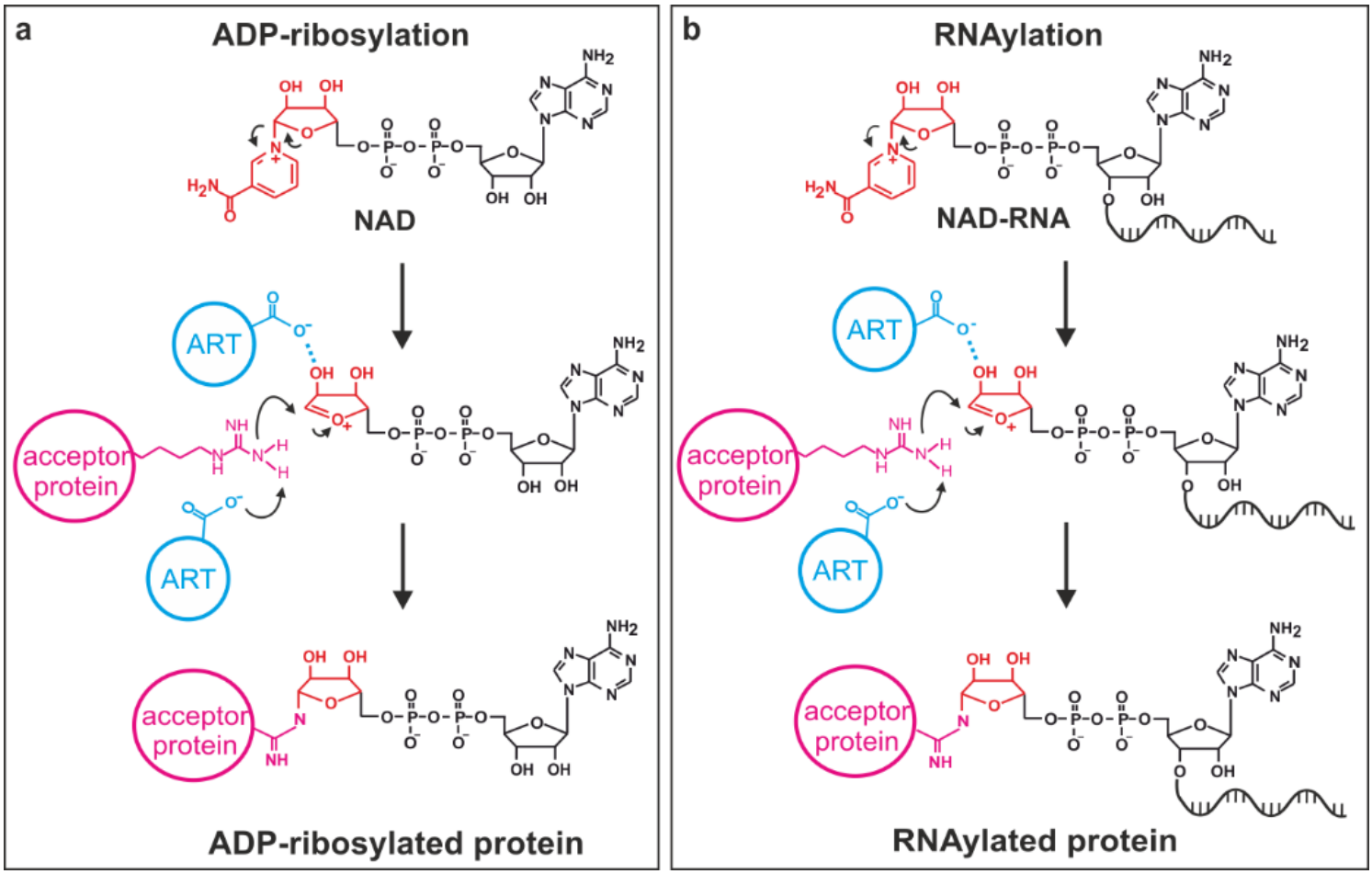

Figure 1

Mechanisms of ADP-ribosylation and proposed “RNAylation”. a. Here, the mechanism of ADP-ribosylation is shown exemplarily for arginine. Initially, the N-glycosidic bond between the ribose and nicotinamide is destabilised by a glutamate residue of an ART. This leads to the formation of an oxocarbenium ion of ADP-ribose. Nicotinamide serves as the leaving group. This electrophilic ion is attacked by a nucleophilic arginine residue of the acceptor protein after glutamate-mediated proton abstraction. This leads to the formation of an N-glycosidic bond 30. b. Analogous to ADP-ribosylation in the presence of NAD, we propose that ARTs might use NAD-RNA to catalyse an “RNAylation” reaction, thereby covalently attaching an RNA to an acceptor protein.

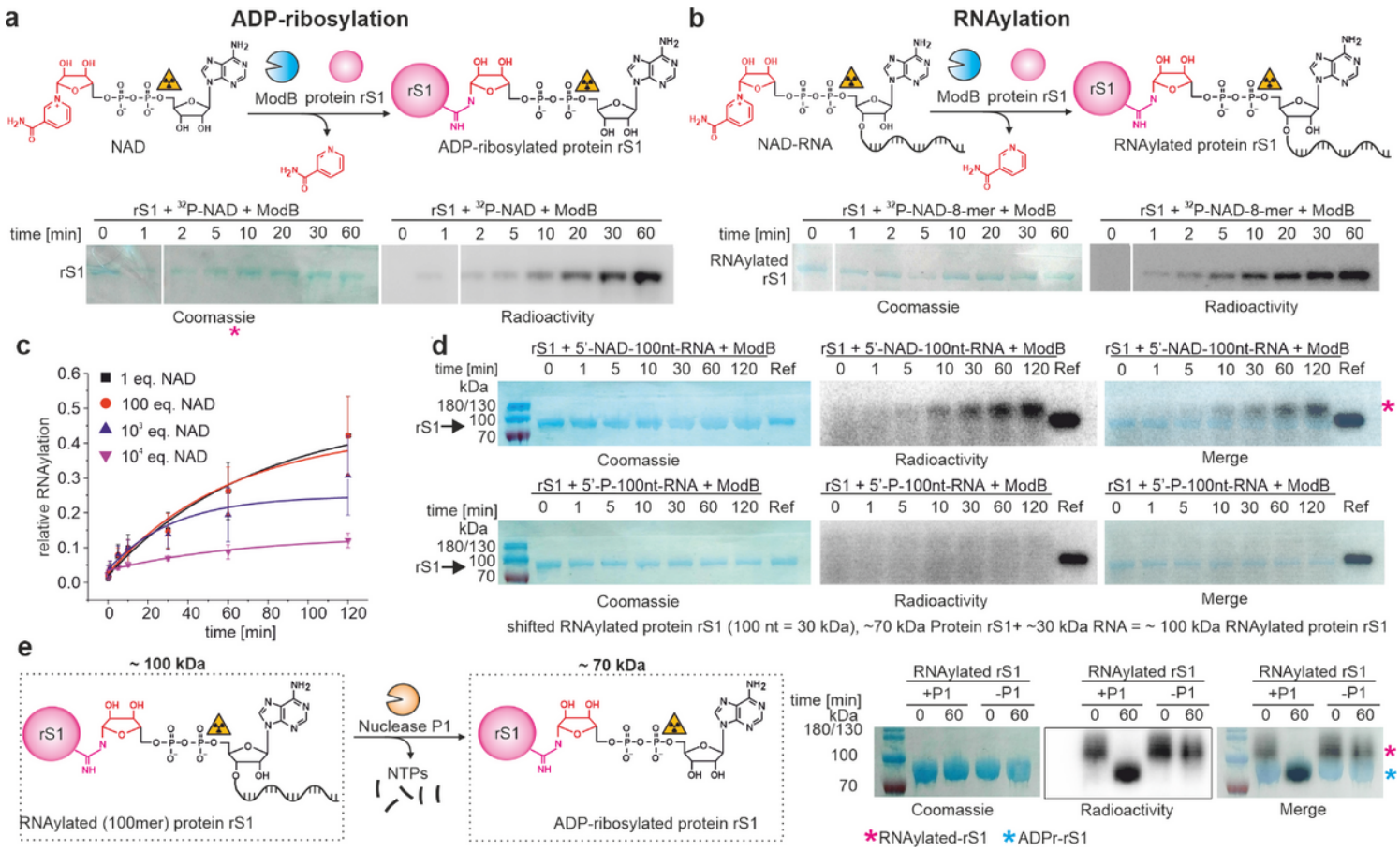

Figure 2

Post-translational protein modification of rS1 by the ART ModB in vitro. a, Time course of the ADP-ribosylation of rS1 by ModB (complete SDS-PAGE gels are shown in Extended Data Fig. 1b). b, Time course of the RNAylation of rS1 by ModB (complete SDS-PAGE gels are shown in Extended Data Fig. 1c). c, in vitro kinetics of the RNAylation of rS1 by ModB in the presence of excess NAD d, in vitro kinetics of the RNAylation of rS1 by ModB using 5'-NAD-100 nt-RNA (Qβ-RNA) as substrate (top panel), analysed by SDS-PAGE. Shifted RNAylated rS1 is highlighted with a pink asterisk. 5'-P-100-nt-RNA is used as a negative control (bottom panel). e, Nuclease P1 digest of RNAylated protein rS1. The covalently attached 100 nt long RNA results in a shift of the RNAylated protein rS1 (~100 kDa) in SDS-PAGE. Treatment of the RNAylated protein rS1 with nuclease P1, which cleaves the phosphodiester bond, resulting in degradation of the attached RNA into mononucleotides. Nuclease P1 can covert RNAylated rS1 into ADP-ribosylated rS1 (~70 kDa), which can be visualised by a downshifted protein band on the SDS-PAGE gel.

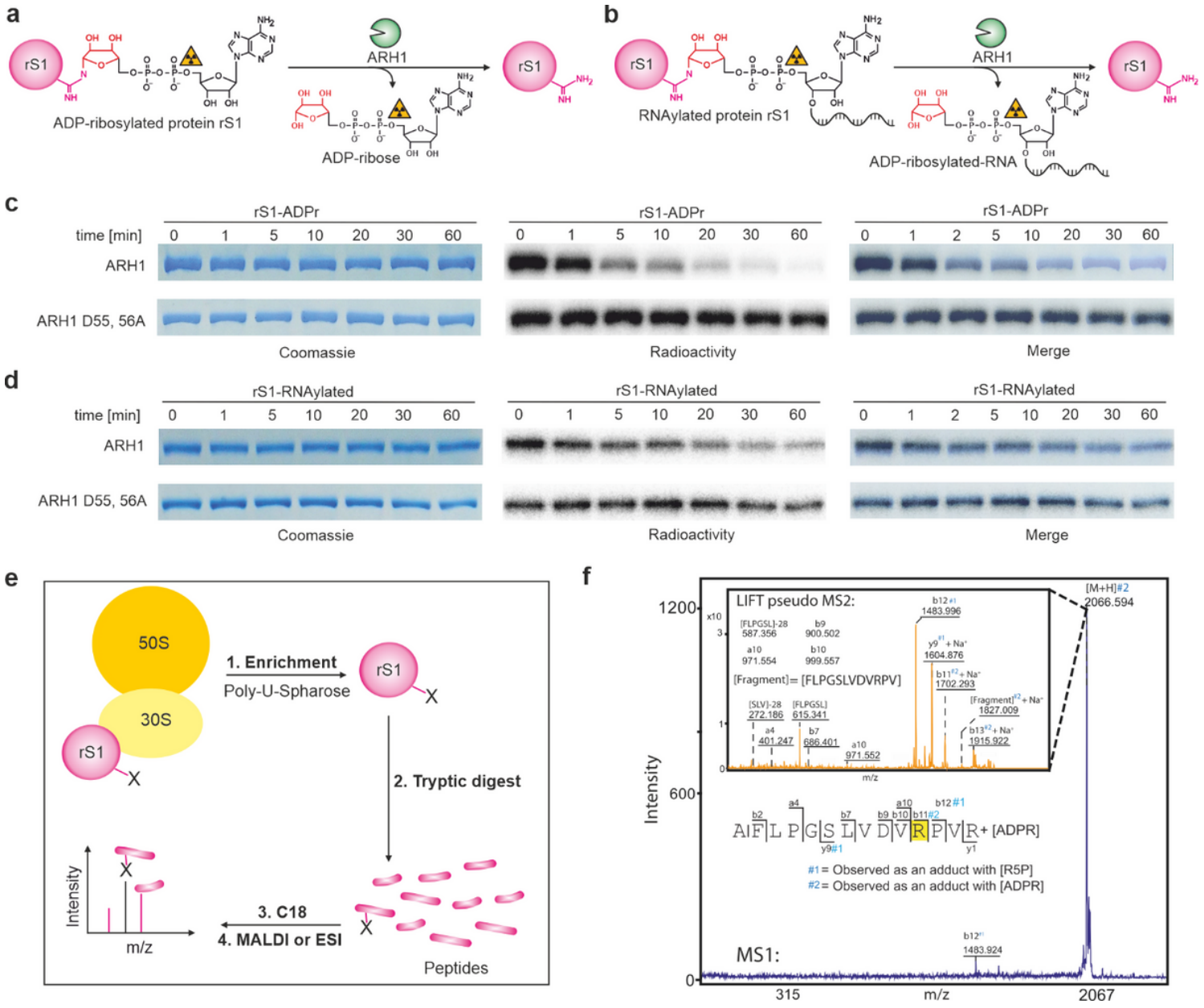

Figure 3

Identification of RNAylation sites of rS1. a-d, Specific removal of ADP-ribosylation and RNAylation by ARH1. Enzyme kinetics of ARH1 in the presence of ADP-ribosylated or RNAylated protein rS1 analysed by SDS-PAGE. e, a pipeline for identifying the modified amino acid residue by mass spectrometry f, MALDI-TOF-MS of in vitro modified protein rS1. Isolation scan (MS1) and pseudo MS2 (LIFT) spectrum of a peptide-ADPR conjugate. The given peptide AFLPGSLVDVRPVR would result in a peak at 2067 if it is linked to ADPR. MALDI-TOF-MS with in vitro modified protein rS1 resulted in the depicted two spectra. LIFT parent ion isolation resulted in the given MS1 with little interference. Note: The shifted b12 ion at m/z = 1483 Th that corresponds to a peptide with R5P modification, indicating the fragile nature of ADP-ribosylations. The resulting pseudo MS2 yields sufficient sequencing ions to confirm the peptide sequence as well as the ADPr modification on the arginine residue boxed in yellow.

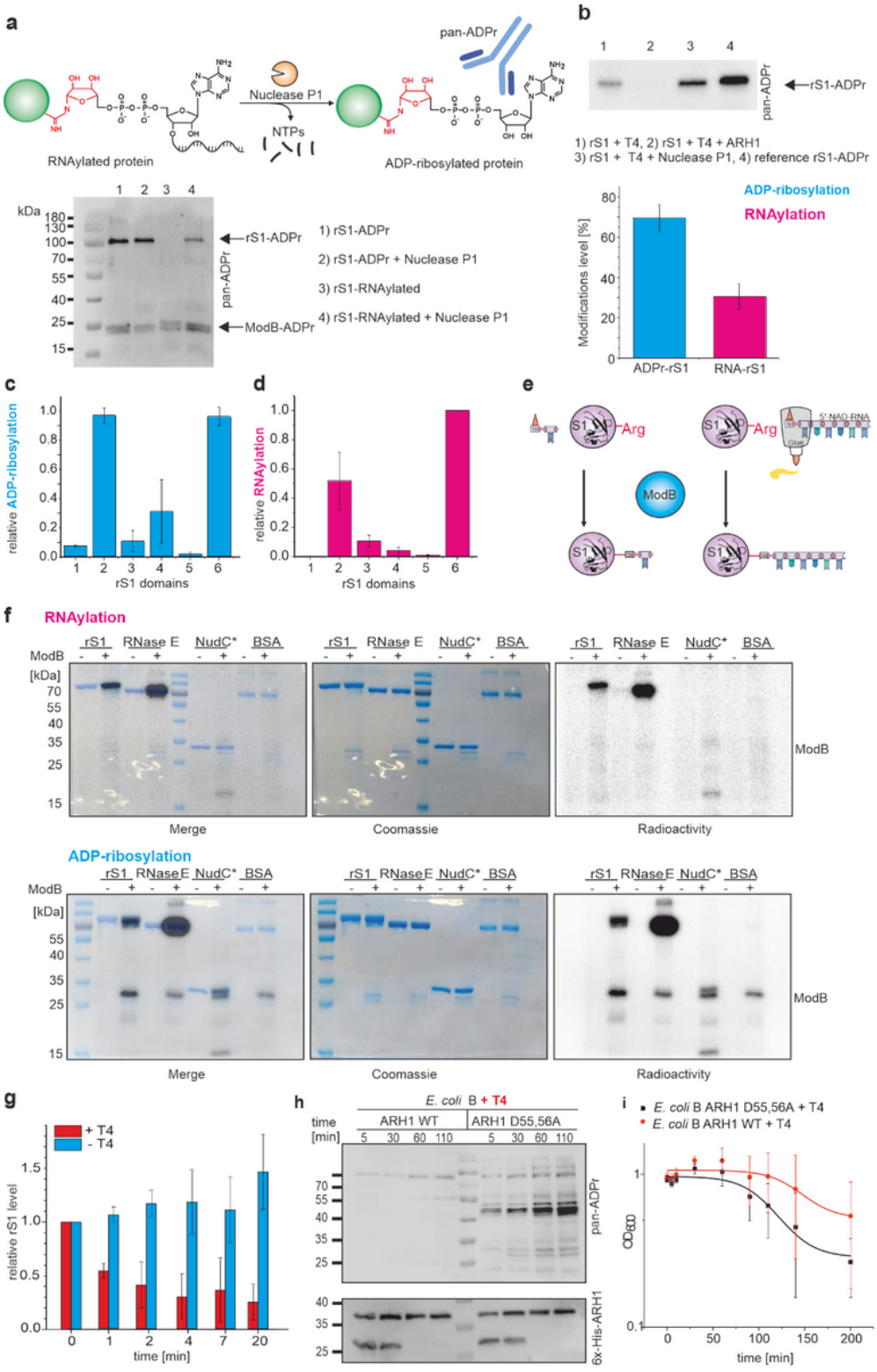

Figure 4

in vivo characterisation of ADP-ribosylation and RNAylation. a, Illustration of the quantification of protein rS1 RNAylation using a nuclease P1 digest and Western Blot analysis. b, Quantification of rS1 RNAylation in vivo. c, Quantification of ADP-ribosylation and d, RNAylation. Modification of rS1 domains 1 – 6. n = 2 of biologically independent replicates. e, Graphical illustration of ADP-ribosylation and RNAylation of proteins carrying a S1-motif by ModB. f, SDS-PAGE analysis of the RNAylation and ADP-ribosylation of

protein rS1, RNase E, inactive NudC mutant (* V157A, E174A, E177A, E178A) and BSA by ModB. n = 2 of biologically independent replicates. g, Quantification of rS1 levels in the presence (+T4) or absence of T4 (-T4), n=4. h, ARH1-mediated removal of ADP-ribosylation and RNAylation modifications during T4 infection. i, Time course of bacteriophage T4-mediated lysis of E. coli expressing a plasmid-borne copy of ARH1–WT or its inactive mutant ARH1 D55,56A.

Supplementary Files

This is a list of supplementary files associated with this preprint. Click to download.

- FinalSI.docx